

AMCoR

Asahikawa Medical College Repository <http://amcor.asahikawa-med.ac.jp/>

Journal of Biological Chemistry (2004. Apr) 279(15):15142–15152.

Neuronal calcium sensor protein visinin-like protein-3 interacts with microsomal cytochrome b5 in a Ca²⁺-dependent manner.

Oikawa, Kensuke ; Kimura, Shoji ; Aoki, Naoko ; Atsuta, Yoshiaki ; Takiyama, Yumi ; Nagato, Toshihiro ; Yanai, Mitsuru ; Kobayashi, Hiroya ; Sato, Keisuke ; Sasajima, Tadahiro ; Tatenno, Masatoshi

**Neuronal Calcium Sensor Protein Visinin-Like Protein-3 Interacts
with Mitochondrial Cytochrome b5 in a Ca²⁺-dependent Manner**

Kensuke Oikawa^{‡**}, Shoji Kimura[§], Naoko Aoki[‡], Yoshiaki Atsuta[¶],
Yumi Takiyama[‡], Toshihiro Nagato[‡], Mitsuru Yanai[‡], Hiroya Kobayashi[‡],
Keisuke Sato[‡], Tadahiro Sasajima[¶], and Masatoshi Tateno[‡]

*From the ‡Department of Pathology, the §School of Nursing, the
¶Department of Surgery, and the †Department of Otolaryngology-Head and
Neck Surgery, Asahikawa Medical College, Asahikawa 078-8510, Japan,*

RUNNING TITLE

Visinin-Like Protein-3 Interacts with Mitochondrial Cytochrome b5

SUMMARY

Visinin-like protein-3, which is one of the neuronal calcium sensors, has been shown to be mainly expressed in cerebellar Purkinje cells, but cellular function of this protein has not yet been elucidated. We examined the tissue distribution of murine visinin-like protein-3 transcripts using real-time reverse transcription-polymerase chain reaction. Visinin-like protein-3 mRNA was found to be expressed in peripheral tissues. Particularly, the expression of the transcript in the thymus was significantly higher than in other peripheral tissues. In addition, B6RVTC1 thymoma cells robustly expressed visinin-like protein-3 mRNA. To identify a target protein of visinin-like protein-3, we performed a pull down experiment using glutathione S-transferase-tagged visinin-like protein-3 and two-dimensional electrophoresis. We demonstrated that microsomal cytochrome b5 was a Ca^{2+} -dependent binding partner of visinin-like protein-3. In a co-immunoprecipitation experiment, it was observed that hippocalcin, as well as visinin-like protein-3, could interact with cytochrome b5. Furthermore, we confirmed that the sequence “V¹¹⁴ – Y¹²⁷” at the C-terminal tail of cytochrome b5 is the minimal structural requirement for binding to visinin-like protein-3. In addition, the loop “H¹⁹ – H²⁵” at the N-terminus of visinin-like protein-3 is essential for binding to cytochrome b5. Microsomal cytochrome b5 was also shown to be a potential activator of cytochrome P450. The present findings raise the possibility that visinin-like protein-3 may link Ca^{2+} -signaling to the machinery of microsomal monooxygenase complex composed of cytochrome b5, cytochrome P450, and some reductases. This paper provides the first evidence of an interaction between visinin-like protein-3 and microsomal cytochrome b5.

INTRODUCTION

Calcium ions play an extremely important and essential role in inter- and intracellular signaling pathways. It is a prominent feature of ions that they regulate diverse cellular processes in many biological systems, including the central nervous system and the immune system. Calcium-binding proteins are thought to mediate the various activities of calcium ions. VILIP-3¹ (Visinin-like protein-3) belongs to the NCS¹ (neuronal calcium sensor) protein family, which includes more than 40 intracellular calcium-sensing proteins expressed primarily in retinal photoreceptors or neurons and neuroendocrine cells (1). The NCS protein family has some common properties as Ca²⁺ sensors and switches. For instance, they show conformational changes after Ca²⁺ binding. They also have two pairs of calcium-binding consensus sequences referred to as EF-hand (EF1, EF2, EF3, and EF4). They also possess a consensus myristoylation sequence at the N-terminal end, the myristoylation of which may be responsible for membrane targeting of NCS proteins in a calcium-dependent manner by a mechanism known as the “calcium-myristoyl switch” (2, 3). The NCS protein family exhibits more than 45% sequence homology and can be grouped into different subfamilies according to the amino acid similarity among various species (1, 4). VILIP-3 belongs to a VILIPs (visinin-like proteins) subfamily, which includes Visinin-like protein-1, Visinin-like protein-2, hippocalcin, and neurocalcin δ in human species (5), as well as in mice. All members of the VILIP subfamily share the major features of NCS proteins described above. There has been some confusion as regards the terminology used for the NCS protein family, as well as that used for VILIPs, because these proteins have been identified in different species and as a result have been renamed several times. To date, there are four synonyms of VILIP-3, including hHLP2 and BDR-1 from humans, NVP-3 from rats and mice, and Rem-1 from chicks. Additionally, the official reference to VILIP-3 in GeneBank is hippocalcin-like 1. VILIP-3 expression was predominantly shown in cerebellar Purkinje cells of humans (6) and

the rat brain (7), as determined by immunohistochemical studies and Western blot analysis. By using *in situ* hybridization, high expression of the VILIP-3 transcript was observed in the cerebellum (Purkinje and granule cells) of the rat brain (8). Unlike other VILIPs in this subfamily, the expression of VILIP-3 mRNA and protein has been confirmed in the peripheral tissues and in cells other than brain cells, although the expression levels were very low. Rat NVP-3 mRNA was detected in the lung, the spleen, and the skeletal muscle (9). Chicken Rem-1 mRNA was detected in the eye, the gut, and hematopoietic cells (10). Rat VILIP-3 protein was detected in the kidney, the spleen, and the testis by Western blot analysis (7). However, the physiological function of VILIP-3 remains unclear. This is the first report that murine VILIP-3 is expressed in the immune system as well as in the neural system. In an attempt to elucidate the cellular function of murine VILIP-3, we attempted to identify proteins with which it interacts, and found that VILIP-3 interacted with mitochondrial cytochrome b5 in a Ca^{2+} -dependent manner. Furthermore, we identified structures required for the interaction between these proteins.

EXPERIMENTAL PROCEDURES

Mice, cells, and culture conditions—C57BL/6 mice (8-10 weeks old) were obtained at our facility and from SLC (Shizuoka, Japan) and were used for RNA samples. The microglia cell line BV2 was a kind gift from Dr. E. Joe (Ajou University, South Korea). Myeloid cell line R453, SP2/0 cell line, mastocytoma cell line P815, monocyte cell line PU5, and macrophage cell line P388D1 are maintained at Memorial Sloan-Kettering Cancer Center, New York, and were made available to our laboratory by Dr. U. Hämmerling. The monocyte cell line M1 was obtained from Riken Gene Bank (Wako, Japan). T cell line 2B4-11 was provided by Dr. R. Abe (NIH, USA). T cell line CTLL-2 was obtained from the American Type Culture Collection (Manassas, VA) and was maintained with exogenous IL-2. Thymoma cell lines EL-4 and B6RVTC1 were provided by Dr. E. Nakayama (Okayama University, Okayama, Japan). The preB cell line 70Z/3 was provided by Dr. C. Paige (University of Toronto, Toronto, Canada). The B cell line A20 was provided by Dr. J. Kappler (University of Colorado, Denver, USA). The cell lines described above were cultured in RPMI 1640 medium (Sigma) supplemented with 10% FCS, 5×10^{-5} M 2-ME, Penicillin, and Streptomycin. Fibroblast cell lines NIH3T3 and 293T, derived from mice and monkeys, respectively, were cultured in Dulbecco's modified Eagle's medium with pyruvate and high glucose (Sigma) supplemented with 5% FCS, 5×10^{-5} M 2-ME, Penicillin, and Streptomycin.

Molecular cloning and expression vectors—p3×FLAG CMV 10 (N-terminal 3×FLAG-tagged protein expression vector) and p3×FLAG CMV 14 (C-terminal 3×FLAG-tagged protein expression vector) were purchased from Sigma. pCMV-Myc (N-terminal c-myc epitope-tagged protein expression vector) and pEYFP-N1(C-terminal EYFP¹-tagged protein expression vector) were purchased from CLONTECH. Mouse VILIP-3¹ cDNA was obtained from mouse spleen cDNA and subcloned into pME18S vector provided by Dr. Maruyama (Tokyo University, Tokyo). GST-V3 (glutathione S-transferase-tagged VILIP-3) expression

vector was made by subcloning VILIP-3 cDNA into the XbaI/XhoI sites of pGEX-KG (11), which was provided by Dr. J. E. Dixon (Purdue University, West Lafayette, IN). V3-F (C-terminal 3×FLAG-tagged VILIP-3) expression vector was obtained by subcloning VILIP-3 cDNA into Hind III/BamHI sites of p3×FLAG CMV 14. V3-Y (EYFP-tagged VILIP-3 of the wild-type) expression vector was constructed by subcloning VILIP-3 cDNA into the Hind III/BamHI sites of pEYFP-N1. HPCA-Y (EYFP-tagged murine hippocalcin) expression vector was obtained by subcloning hippocalcin cDNA derived from mouse brain cDNA, into the Hind III/BamHI sites of pEYFP-N1. Mouse cytochrome b5 cDNA was obtained by PCR using B6RVTC1 cDNA. M-b5 (myc-tagged cytochrome b5 of the wild-type) expression vector was obtained by subcloning the PCR product into the EcoRI/XhoI sites of pCMV-Myc. F-b5 (N-terminal 3×FLAG-tagged cytochrome b5) expression vector was constructed by subcloning the PCR product into the EcoRI/BamHI sites of p3×FLAG CMV 10. GST-b5 (glutathione S-transferase-tagged cytochrome b5) expression vector was obtained by subcloning the PCR product into the EcoRI/Hind III sites of pGEX-KG. All constructs were confirmed for their sequences by automated sequencing. The abbreviations for the constructs of the wild-type, described above, are summarized in Fig. 2 with their schematic representations.

Constructions of mutants and truncated-form protein expression vectors—VILIP-3 derivatives: V3-Y expression vector, described above, was used as either a template for PCR and for mutagenesis in all constructions. V3ΔN14-Y and V3ΔN25-Y (EYFP-tagged VILIP-3 truncated of N-terminal ~14 and ~25 residues) expression vectors were obtained by subcloning the PCR products into the HindIII/BamHI sites of pEYFP-N1. V3ΔH19~H25-Y (EYFP-tagged VILIP-3 deleted residues “H19—H25”) expression vector was constructed by using a PCR overlap extension technique (12). The truncated amino acid sequences of VILIP-3 are shown in Fig. 7A. The abbreviations used for the truncated constructs of VILIP-3 are

summarized in Fig. 2B with their schematic representations. G2A (Gly²→Ala mutant of VILIP-3-EYFP) expression vector was obtained by subcloning the PCR product into pEYFP-N1. Other derivatives (T23I, Thr²³→Ile mutant; H42D, His⁴²→Asp mutant; L43Y, Leu⁴³→Tyr mutant; L43P, Leu⁴³→Pro mutant; T44E, Thr⁴⁴→Glu mutant; T44A, Thr⁴⁴→Ala mutant; V45E, Val⁴⁵→Glu mutant) of V3-Y expression vectors were constructed by using a Transformer Site-Directed Mutagenesis Kit (CLONTECH) or Mutan-Super Express Km Kit (TaKaRa Biomedicals). Cytochrome b5 derivatives: DNA fragments encoding C-terminal truncated cytochrome b5 were obtained by PCR using a M-b5 expression vector as a template. M-b5ΔC15 and M-b5ΔC7 (myc-tagged cytochrome b5 truncated C-terminal ~15 and ~7 residues) expression vectors were obtained by subcloning PCR products into the EcoRI/XhoI sites of pCMV-Myc. GST-b5ΔC21, GST-b5ΔC15, and GST-b5ΔC7 (GST-tagged cytochrome b5 truncated C-terminal ~21, ~15, and ~7 residues) expression vectors were obtained by subcloning PCR products into the EcoRI/XhoI sites of pGEX-KG. GST-b5ΔA120~Y127 (GST-tagged cytochrome b5 deleted sequence “A¹²⁰—Y¹²⁷”) was constructed by using a PCR overlap extension technique. The PCR product was subcloned into the EcoRI/XhoI sites of pGEX-KG. GST+V114~Y127 and GST+A120~Y127 (GST-tagged peptides of C-terminal tail of cytochrome b5, “V¹¹⁴—Y¹²⁷” and “A¹²⁰—Y¹²⁷”) expression vectors were created by adding short DNA sequences encoding each corresponding sequence into the EcoRI/XhoI sites of pGEX-KG. The truncated and additional C-terminal amino acids of cytochrome b5 are shown in Fig. 6A. The abbreviations used for cytochrome b5 derivatives are summarized in Fig. 2A with their schematic representations. The BL21 *E. coli* (Invitrogen), transformed by GST-tagged cytochrome b5 mutant expression vectors, were grown in 2 ml of LB medium containing 50 μg/ml ampicillin at 37°C to an O.D. of 575=0.3-0.5. Following the addition of 10μl of 0.1M IPTG¹ (Isopropyl-1-thio-β-D-galactoside) (final 0.5mM) to the culture medium, and the induced cells were

grown for an additional 3-4 h at 25°C. The expressed proteins were purified from bacterial sonicates using GS4B¹ (Amersham Pharmacia Biotech AB), and the proteins were eluted with free glutathione. The concentrations of proteins in the eluates were assessed by SDS-PAGE, and approximately 1µg of purified proteins were used for the co-immunoprecipitation assay.

RNA source, total RNA extraction, and reverse transcription—The total RNAs were extracted from the mouse tissues and cell lines using Sepazol reagent (Nacalai Tesque, Tokyo, Japan) according to the manufacturer's protocol. cDNA was synthesized using a 1st-Strand cDNA Synthesis Kit for RT-PCR AMV (Roche) and 1µg of total RNA was used as a template. The accompanying random primer pdN₆ was used for the reactions. The procedures used for the reactions followed the manufacturer's recommendations.

Relative quantification of mouse VILIP-3 mRNA—The expression of VILIP-3 mRNA in tissues and cells was analyzed by two-step real-time RT-PCR using the LightCycler-DNA Master SYBR Green I (Roche). β-actin and GAPDH was used as reference genes for the tissue examination and the cell line examination, respectively. The following primers were used for mouse VILIP-3 (forward primer, ACACACGGAATTCACCGACCAT; reverse primer, ACACACGGAATTCACCGACCAT), β-actin (forward primer, ACCCACA CTGTGCCCATCTA; reverse primer, CGGAACCGCTCATTGCC), and GAPDH (glyceraldehyde phosphate dehydrogenase: forward primer, CGGAACCGCTCATTGCC; reverse primer, CGGAACCGCTCATTGCC). For quantification, an external calibration curve was used. VILIP-3, β-actin, and GAPDH PCR products amplified by each primer pair were cloned separately in pCR2.1 vector (Invitrogen). Dilutions of each plasmid containing from 10⁴ to 10⁸ dsDNA molecules were used as standard templates for the production of external calibration curves. The conditions for RT-PCR were optimized by a LightCycler instrument (Roche) with regard to the MgCl₂

concentrations, annealing temperatures, elongation time, and fluorescence acquisition temperatures. PCR amplifications were repeated in triplicate. The PCR efficiencies (E) were calculated according to the following equation: $E=10^{-1/\text{slope}}$. Each mean slope of each external calibration curve was used as a representative slope value. CP (Crossing point) for each transcript were determined by the “Fit Point Method” performed in the LightCycler software 3.3 (Roche). The average of each of the triplicate CP values was used as a representative CP value. Relative quantification ratios of each tissue type and cell line were calculated according to the following equation: $\text{ratio}=(E_{\text{target}})^{\Delta\text{CP}_{\text{target}}(\text{control-sample})}/(E_{\text{ref}})^{\Delta\text{CP}_{\text{ref}}(\text{control-sample})}$. E_{target} indicates the PCR efficiency when using the VILIP-3 primer and the standard template of VILIP-3. E_{ref} refers to the PCR efficiency when reference gene (β -actin or GAPDH) primer pairs and standard templates were used. $\Delta\text{CP}_{\text{target}}$ (control-sample) and $\Delta\text{CP}_{\text{ref}}$ (control-sample) refer to the CP deviation of each tissue type or cell line versus a control tissue (the brain) or a control cell line (BV2) for the VILIP-3 transcripts and the reference gene transcripts, respectively (13).

GST pull-down experiment—TOP10 *E. coli* (Invitrogen) transformed by GST-V3 expression vector or PGEX-KG were grown in 2 ml of LB medium containing 50 $\mu\text{g/ml}$ ampicilin at 37°C to an O.D.of 575=0.3-0.5. Following the addition of 10 μl of 0.1M IPTG (final 0.5mM) to the culture medium, and the induced cells were grown for an additional 3-4 h at 37°C, pelleted, washed once with PBS, resuspended in 400 μl PBS containing 1% Triton-X100, and the protease inhibitor cocktail Complete Mini EDTA free (Roche); the cells were then subjected to freeze-thaw cycles (3 \times) using liquid nitrogen. The cell lysates were clarified by centrifugation at 17000 $\times\text{g}$ for 30 minutes and were stored at -80°C until needed for further use. The concentration of bait protein (GST¹ or GST-V3) among the lysates was assessed by SDS-PAGE. For the analysis of affinity precipitations, cell lysates were prepared using a B6RVTC1 thymoma cell line. 1×10^8 cells of B6RVTC1 were harvested and lysed in 1 ml of

lysis buffer (75 mM HEPES¹ (pH7.5), 100 mM NaCl, 100 mM (NH₄)₂SO₄, 1 mM CaCl₂ or EGTA, 0.5% CHAPS¹, and 0.1 mM DTT) containing the protease inhibitor cocktail Complete Mini EDTA free (Roche) for 1 h at 4°C. Transformed *E. coli* lysates containing approximately 10µg of bait proteins were added to the B6RVTC1 lysates. The mixture was incubated for 24 h at 4°C. Then, a 5µl bed volume of GS4B beads equilibrated by applying lysis buffer with or without calcium was added to the mixture, and the mixture was incubated for 1 h at 4°C. Finally, the beads were washed extensively in the appropriate lysis buffer, dried for a few minutes using a Speed Vac, and stored at -30°C until use.

2-DE (two-dimensional electrophoresis) and amino acid sequence—The MultiphorTM II isoelectric focusing systems, IPG strips (3-10L, 11cm), IPG-buffer (pH 3-10L), ExcelGel SDS (gradient 8-18%), ExcelGel SDS buffer strips, and the Plus One Silver Staining Kit were purchased from Amersham Pharmacia Biotech AB. Prior to isoelectric focusing, IPG strips were rehydrated with sample buffer (8M Urea, 2% CHAPS, 0.5% IPG buffer (pH3-10L), 18 mM DTT) for 12 h. After IPG strip rehydration, proteins bound to GS4B, prepared as described above, were eluted with sample buffer, and loaded onto IPG strips. 2-DE were performed according to the manufacturer's instructions. To visualize proteins resolved by 2-DE, silver staining of 2-DE gels was performed. Gels containing area of interest were stained with Coomassie Brilliant Blue; then, a spot of interest was selected and digested with trypsin for 16 h at 35°C. The peptide fragments generated in this manner were separated using reverse-phase HPLC. The fragments were analyzed by a protein sequencer and confirmed sequences were identified by homology searches of a CD database.

Transfection—LipofectAMINE reagent (Invitrogen) was used for transfection of 293T cells. For the co-immunoprecipitation experiments, 70-80% confluent 293T cells in one well of a 6-well plate were transfected using 1µg of 3×FLAG-tagged protein expression vectors and 1µg of c-myc epitope or EYFP-tagged protein expression vectors. For the *in vitro* binding assay

using GST-tagged cytochrome b5 mutants, 70-80% confluent 293T cells in one well of a 6-well plate were transfected by 2 μ g of V3-F expression vector.

Co-immunoprecipitation, electrophoresis, and Western blotting—Transfected cells in one well of a 6-well plate were lysed in 1 ml of lysis buffer (0.5% CHAPS, 50 mM HEPES (pH 7.5), 300 mM NaCl, and 1 mM CaCl₂ or EGTA) containing the protease inhibitor cocktail Complete Mini EDTA free (Roche). The lysates were clarified by centrifugation and immunoprecipitated with anti-FLAG M2 agarose beads (Sigma) for 1-2 h at 4°C. The immunocomplexes were washed and eluted with 3 \times FLAG peptide (Sigma) solution. The eluted samples were loaded on 4-12% NuPage bis-Tris SDS-PAGE gels (Invitrogen) under reducing conditions. The resolved proteins were then blotted onto Immobilon-P (Millipore, Bedford, MA), blocked in 5% skim milk, and probed with each primary antibody, followed by incubation with the corresponding HRP-conjugated secondary antibody. ECL or ECL⁺ Western blotting detection reagents (Amersham Pharmacia Biotech AB) were used for detection. The following primary antibodies were used: anti-c-Myc (CLONTECH) for the detection of M-b5 and M-b5 derivatives, anti-GST (Amersham Pharmacia Biotech AB) for the detection of GST-b5 and GST-b5 derivatives, and anti-EYFP (anti-Living-color AV peptide antibody) (CLONTECH) for the detection of V3-Y, HPCA-Y and V3-Y mutants.

RESULTS

Expression pattern of VILIP-3 mRNA in mouse tissues and cell lines—The tissue distributions of VILIP-3 in several species have been reported in recent years, as noted above in the introduction. However, there has not yet been a report of VILIP-3 expression in mice. Here, we examined the tissue distribution of murine VILIP-3 using real-time RT-PCR. VILIP-3 mRNA was highly expressed in the brain and the eye. In the peripheral tissues, ubiquitous expression of VILIP-3 mRNA was observed, although the expression levels were low. In addition, the expression level of the VILIP-3 transcript was relatively high in the thymus (relative expression ratio: 0.39) compared to that of the other peripheral tissues (Fig. 1A). In contrast to VILIP-3 expression, the expression of hippocalcin mRNA was high in the brain, but was not detected in any of the same series of peripheral tissues (Data not shown). In a similar manner, we examined the expression of VILIP-3 mRNA in several cell lines including immunocyte lines, NIH3T3, and microglia cell line BV2. The expression levels of VILIP-3 transcripts in monocytic cell lines PU5 and M1, macrophage cell line P388D1, T cell line 2B4-11, thymocyte cell line EL-4, NIH3T3, and BV2 were relatively high compared to the levels in lymphocytic cell lines CTLL-2, SP2/0, 70Z/3, and A20. Moreover, the VILIP-3 expression in B6RVTC1 cells originating from thymoma cells was more than 3-fold higher than that of other cell lines (Fig. 1B).

Search for a target protein of VILIP-3—In order to identify a Ca²⁺-dependent binding partner of VILIP-3, we performed a GST pull-down experiment by using GST-VILIP-3 fusion protein and B6RVTC1 cell lysates. Fig. 3 shows the 2-DE gel protein profiles. The distinct spot (a), which appeared only in the presence of calcium, was detected in silver-stained 2-DE gels (Fig. 3A). The molecular weight and isoelectric point of the spot were approximately 16-kDa and 5.2, respectively. Spot (a), detected on the Coomassie Brilliant

Blue (CBB) stained gel (Fig. 4A), was selected and subjected to an analysis of internal amino acid sequences using in-gel digestion and peptide fingerprinting methods. Two of the significant peptide fragments were submitted to amino acid sequence analysis, and the sequences were identified with N-terminal sequences involved in a highly conserved heme-binding domain of mitochondrial cytochrome b5 of many species (Fig. 4B). Therefore, we confirmed that spot (a) was endogenous murine mitochondrial cytochrome b5. In order to provide independent evidence for the interaction between VILIP-3 and mitochondrial cytochrome b5 detected above, we performed a co-immunoprecipitation assay. 293T cells were transiently co-transfected with V3-F (C-terminal 3×FLAG-tagged VILIP-3) expression vector and M-b5 (myc-tagged cytochrome b5 of the wild-type) expression vector. The immunoprecipitated complexes bound to anti-FLAG antibody were analyzed for the presence of M-b5 by Western blotting. Fig. 5A shows that M-b5 bound specifically to V3-F and that the interaction arose only in the presence of calcium. This interaction was also observed in a co-immunoprecipitation assay using 293T cells transfected with V3-Y (EYFP-tagged VILIP-3 of the wild-type) expression vector and F-b5 (N-terminal 3×FLAG-tagged cytochrome b5) expression vector. When the constructs were co-expressed, V3-Y was detected by Western blot analysis for immunoprecipitated complex bound to anti-FLAG antibody in the presence of calcium, but not in the absence of calcium (Fig. 5B). These data show that VILIP-3 interacts specifically with mitochondrial cytochrome b5 in a calcium-dependent manner.

Identification of the minimal structural requirements of mitochondrial cytochrome b5 for the interaction with VILIP-3—Cytochrome b5 is a small, cylindrical, acidic membrane protein consisting of 6 helices and 5 β -strands (14). The protein is folded into two domains, namely, a globular hydrophilic domain and a smaller hydrophobic domain. The globular domain is a cytosolic heme-containing, amino-terminal, hydrophilic region, whereas the smaller domain is the hydrophobic, membrane-binding carboxyl portion of 14-18 residues, which are

connected in turn to the globular domain by a proline-containing hinge region of ~7 amino acids and followed by 7 polar amino acids at the very end of the polypeptide chain (15). To determine whether the amino-terminal globular domain or the carboxyl terminal membrane-binding domain of cytochrome b5 is involved in binding to VILIP-3, we carried out a co-immunoprecipitation assay by using carboxyl terminal-truncated constructs of cytochrome b5. Although M-b5 Δ C7 (myc-tagged cytochrome b5 truncated C-terminal ~7 residues), as well as M-b5 (myc-tagged cytochrome b5 of the wild-type), were able to bind to VILIP-3, M-b5 Δ C15 (myc-tagged cytochrome b5 truncated C-terminal ~15 residues) was not able to carry out this interaction (Fig. 6B). We also performed an *in vitro* binding assay by using affinity-purified GST-tagged cytochrome b5 mutants and V3-F (C-terminal 3 \times FLAG-tagged VILIP-3) bound to anti-FLAG agarose beads. Fig. 6C shows that when more than 15 amino acid residues at the end of the carboxyl terminus of cytochrome b5 were deleted, it was unable to bind to VILIP-3. Interestingly, the signal of GST-b5 Δ C7 (GST-tagged cytochrome b5 truncated C-terminal ~7 residues) was more intense than that of GST-b5 (GST-tagged cytochrome b5 of the wild-type) sample (Fig. 6C). Therefore, 7 polar amino acids at the very end of the carboxyl terminus appeared to inhibit the interaction between VILIP-3 and cytochrome b5. In addition, GST-b5 Δ A120~Y127 (GST-tagged cytochrome b5 deleted sequence “A¹²⁰—Y¹²⁷”) could not bind to VILIP-3, suggesting that the sequence “A¹²⁰—Y¹²⁷” at the carboxyl terminal end of cytochrome b5 is necessary for binding to VILIP-3. To determine whether or not this sequence is the minimal structural requirement for binding, we performed another immunoprecipitation assay using GST-polypeptides of cytochrome b5 fusion constructs. While GST+A120~Y127 (GST-tagged peptide of C-terminal tail of cytochrome b5 “A¹²⁰—Y¹²⁷”) was not able to bind to VILIP-3, GST+V114~Y127 (GST-tagged peptide of C-terminal tail of cytochrome b5 “V¹¹⁴—Y¹²⁷”) did interact with VILIP-3 (Fig. 6D), providing evidence that the sequence “V¹¹⁴—Y¹²⁷” at the hydrophobic membrane-

anchoring domain of cytochrome b5 is essential and sufficient for the interaction with VILIP-3.

Identification of the structural requirements of VILIP-3 for binding to cytochrome b5—The three-dimensional structure of the NCS proteins and the conformational changes that occur upon Ca^{2+} binding have been extensively characterized in a study of bovine recoverin, which was the first NCS protein to be identified. Comparison of the Ca^{2+} -free form with the Ca^{2+} -bound form of recoverin demonstrated extensive conformational changes due to Ca^{2+} binding (3). The Ca^{2+} -free form has a compact structure with the myristoyl group buried within a hydrophobic pocket formed by residues within EF-1 and hydrophobic residues contributed by other helices. In the Ca^{2+} -bound form, the myristoyl group flips out into the aqueous solution, leaving an exposed hydrophobic surface potentially able to interact with a target protein. In addition, the N-terminal domain is rotated relative to the C-terminal domain in the Ca^{2+} -bound form. The C-terminal domain is relatively unaffected. The major conformational changes in Ca^{2+} -bound recoverin occur as a result of rotation of the backbone at residues Gly⁴¹ within EF-1 and Gly⁹⁵ between EF-2 and EF-3. These two residues are conserved in all of the NCS proteins (4). It was suggested, therefore, that similar conformational changes should occur in VILIP-3 following Ca^{2+} -binding. In support of this idea, the crystal structure of bovine neurocalcin δ , which has 90% identity with VILIP-3 in the Ca^{2+} -bound form, is very similar to that of Ca^{2+} -bound recoverin (16). Therefore, it was speculated that the structural requirements of VILIP-3 for binding to cytochrome b5 most likely would be found in the N-terminal extension. Hippocalcin, which has 94% identity with VILIP-3, is the most similar to VILIP-3 among the VILIP subfamily of proteins, and possesses seven amino acid residues out of twelve that differ from the amino acid sequences of VILIP-3 at the N-terminal region from the very end of the N-terminus to EF-1. The pair-wise alignment of the N-terminal amino acid sequences of VILIP-3 and hippocalcin are shown in Fig. 7A. In order to

determine the importance of the N-terminus of VILIP-3 for the interaction with cytochrome b5, we obtained murine hippocampal cDNA from brain cDNA, and performed a co-immunoprecipitation experiment using EYFP-tagged hippocampal cDNA. A Ca^{2+} -dependent interaction between hippocampal cDNA and cytochrome b5 was observed (Fig. 5B). However, comparing the signal intensity of HPCA-Y (EYFP-tagged mouse hippocampal cDNA of the wild-type) and V3-Y, the binding of hippocampal cDNA to cytochrome b5 was approximately 1.3-fold more intensive than that of VILIP-3 to cytochrome b5. The region “H¹⁹ – H²⁵” of VILIP-3, as well as the region “N¹⁹ – L²⁵” of hippocampal cDNA, is thought to form a loop within the $\alpha\alpha$ folding unit at the N-terminus, based on the three-dimensional structure of bovine neurocalcin δ and the predicted secondary structure obtained by PROFsec available on the web. VILIP-3 possesses residues that differ from those of hippocampal cDNA at the N-terminal loop and EF-1. GCAP-2, an NCS protein family member, interacts with guanylyl cyclase and regulates enzymatic activity. It has been shown that GCAP-2-specific amino acid residues within EF-1 can create a contact surface for binding of GCAP-2 to the cyclase (17). We speculated that the distinct cytochrome b5-binding affinity of the two proteins occurs due to differences between amino acid residues at the N-terminal loop and EF-1; these findings indicate that there is most likely a contact surface that interacts with cytochrome b5 at these regions. To determine whether VILIP-3 interacts with cytochrome b5 through EF-1, we probed the EF-1 region of VILIP-3 by a co-immunoprecipitation assay using V3-Y mutants, which have a single mutation in the EF-1 region. The substituted residues within EF-1 are shown in Fig. 7A. The interaction between VILIP-3 and cytochrome b5 was unaffected by any of the substitutions within EF-1 (Fig. 7B). According to the results of a structural analysis by PROFsec, the substitution of Thr²³ with Ile would change the structure from a loop to a helix at this point. T23I (EYFP-tagged Thr²³→Ile mutant of VILIP-3) was found to bind to cytochrome b5 less intensively in this case (Fig. 7B). Furthermore, while V3 Δ N25-Y (EYFP-

Vsinin-Like Protein-3 Interacts with Mitochondrial Cytochrome b5

tagged VILIP-3 truncated N-terminal ~25 residues) exhibited a weak association with cytochrome b5, V3ΔH19~H25-Y, which was subjected to deletion of the loop around Thr²³, was unable to bind to cytochrome b5 (Fig. 7C). These results imply that the N-terminal loop region of VILIP-3 “H¹⁹ – H²⁵” is involved in the interaction with cytochrome b5. G2A (EYFP-tagged Gly²→Ala mutant of VILIP-3) and V3ΔN14-Y (EYFP-tagged VILIP-3 truncated N-terminal ~14 residues), which are thought to be unmyristoylated, were also bound to cytochrome b5 (Fig. 7B). These results indicated that the N-terminal myristoylation of VILIP-3 was not necessary for binding to cytochrome b5 *in vitro*.

DISCUSSION

The results of our analysis of VILIP-3 expression in tissues, carried out by real-time RT-PCR, were found to be similar to those reported for other species (8, 9). Interestingly, in the thymus, slightly higher expression of VILIP-3 was observed in comparison with that in other peripheral tissues. In addition, the thymoma cell line B6RVTC1 robustly expressed VILIP-3. Hippocalcin is known to have 94% identity with VILIP-3 and a highly restricted tissue distribution. In contrast to hippocalcin, VILIP-3 has a ubiquitous distribution, suggesting that it may possibly play a role not only in the central nervous system, but also in the peripheral tissues, particularly in the thymus.

To our knowledge, this is the first report to identify the Ca^{2+} -dependent binding partner of VILIP-3. Using a GST-pull down experiment in conjunction with 2-DE and N-terminal amino acid sequencing, we confirmed that VILIP-3 was able to associate with mitochondrial cytochrome b5 in a calcium-dependent manner. Moreover, in a co-immunoprecipitation assay, it was found that a Ca^{2+} -dependent interaction occurred between hippocalcin and cytochrome b5. Mitochondrial cytochrome b5 is one of the known heme-binding proteins and functions as an electron carrier for several membrane-bound oxygenases such as cytochrome P450 (18, 19). Three major isozymes of cytochrome b5 are known to exist. One of these is mitochondrial cytochrome b5, located in the endoplasmic reticulum. The second is mitochondrial cytochrome b5, which arises from a distinct mitochondrial-type gene. The subcellular localization of the mitochondrial type is the outer membrane of mitochondria. While the heme peptide region of the mitochondrial type is 54% identical to that of the mitochondrial type, the identity of their carboxyl terminal regions is only 25% in mice. The third isozyme is a soluble form of cytochrome b5 found in erythrocytes, and appears to be a splice variant of the mitochondrial type, although it lacks the membrane-binding carboxyl terminus. In addition to these isozymes, there are fusion enzymes containing cytochrome b5 as a component,

including mitochondrial sulfite oxidase (20, 21), the $\Delta 5$ - and $\Delta 6$ -fatty acid desaturases (22, 23), and b5+b5R (24). In the present GST pull-down assay, it was found that spot (a), which was only detected in the presence of calcium, shared the molecular weight, the isoelectric point, and the confirmed N-terminal amino acid sequences with those of the microsomal type as distinct features. As demonstrated here, the VILIP-3 binding region of cytochrome b5 is in the membrane-binding carboxyl terminus, and the soluble form of cytochrome b5 is considered unable to bind to VILIP-3. Recently, calcium-induced translocation to the perinuclear region has been observed in the case of rat hippocalcin and neurocalcin δ (25, 26). VILIP-3 is likely to have the same ability to translocate, depending on the increase in the intracellular Ca^{2+} concentration; moreover, the present findings suggest that Ca^{2+} -dependent target proteins exist in the perinuclear region. Therefore, microsomal cytochrome b5, which is located in the endoplasmic reticulum - perinuclear region, is well suited as a Ca^{2+} -dependent binding partner of VILIP-3.

In the present study, we confirmed that the region “V¹¹⁴ – Y¹²⁷,” at the C-terminal membrane-binding domain of cytochrome b5 is the minimal essential structure for the interaction with VILIP-3. The function of the membrane-binding domain of cytochrome b5 is believed to be the anchoring of cytochrome b5 to the membrane of the endoplasmic reticulum by its hydrophobic stretch of ~23 amino acids, and this region is thought to orient the catalytic site at the membrane-aqueous interface to permit rapid electron transfer (27, 28). It has been known that cytochrome b5 is synthesized on cytosolic ribosomes and is post-translationally inserted into the microsomal membranes independent of signal recognition particles (29, 30). Although the ten C-terminal residues are thought to be essential for targeting to the membrane (31), it is not known whether the insertion into the membrane occurs spontaneously or by a receptor-mediated mechanism. In some attempts to elucidate the machinery of targeting the protein into the membrane, two different modes of binding to

artificial liposomes have been demonstrated *in vitro*. A “loose-binding form” is obtained when cytochrome b5 is mixed with preformed liposomes (32). Alternatively, in the presence of detergent, a “tight-binding form” is obtained (33). To date, two different models of conformation have been proposed for the membrane-binding domain: 1) a single membrane-spanning helix and 2) a hairpin-type structure, which would result from isomerization of the trans Ile¹¹⁴Pro¹¹⁵ amide bond to the cis amide bond; the membrane-binding domain is thought to span only half of the bilayer in this case (Fig. 4C) (34). A few studies have suggested that the tight-binding form might represent a membrane-spanning conformation (19, 35–37). No examples of stable integral membrane protein structures that span only one-half of the bilayer in a hairpin conformation have been identified in the high-resolution X-ray structures of the membrane proteins determined to date. However, it has been reported in one study that the tight-binding form is a hairpin conformation (33), and other studies have suggested that both the tight and loose forms are hairpin structures (38). In addition, computer modeling of the three-dimensional structure of full-length cytochrome b5 has indicated that the membrane-bound part forms a loop structure (39). In another paper, it was shown that the peptide could flip between two alternative conformations under conditions of changing temperature (40). Thus, the topology of the membrane-binding domain still remains to be determined. Interestingly, the VILIP-3 binding sequence of cytochrome b5 indicated in this study included a Pro¹¹⁵ residue. As VILIP-3 exists in cytosol, it is possible that a hairpin-loop conformation may be more accessible to VILIP-3 than a single-helix transmembrane conformation, assuming that the helix following Pro¹¹⁵ within the VILIP-3 binding region exists on the cytosolic side of the bilayer in a hairpin-loop conformation (Fig. 4C). In any case, as it is clear that the VILIP-3 binding sequence of cytochrome b5 exists within the membrane of the ER¹, the interaction between VILIP-3 and cytochrome b5 must occur within the hydrophobic core of the membrane.

We also confirmed that the N-terminal loop “H¹⁹ – H²⁵” of VILIP-3 was necessary for binding to cytochrome b5. However, the hydrophilic loop region, without any assistance, is not likely to be integrated into the hydrophobic core of the ER membrane and not directly attach to the C-terminal hydrophobic tail of cytochrome b5. We take note of the very hydrophobic helix “L⁸⁹ – G⁹⁵” lying between EF-2 and conserved Gly⁹⁵, which is known to be a point of rotation following Ca²⁺-binding. In the analysis of hydrophobicity, the region “L⁸⁹ – G⁹⁵” exhibited the most pronounced hydrophobicity throughout the full length of VILIP-3 (Fig. 8). According to the three-dimensional structure of Ca²⁺ bound form of bovine neurocalcin δ , which has a similar hydrophobic profile to that of VILIP-3 (Fig. 8), the helix “L⁸⁹ – G⁹⁵” is adjacent to the N-terminal loop “S¹⁹ – H²⁵”, corresponding to the loop “H¹⁹ – H²⁵” in VILIP-3. A compact and amphipathic structure, involving the N-terminal hydrophilic loop “S¹⁹ – H²⁵” and the hydrophobic helix “L⁸⁹ – G⁹⁵”, must be created at the surface of Ca²⁺ bound neurocalcin δ (Fig. 9). Interestingly, Asp²¹ adjoins to Arg⁹⁴ in the local environment within the amphipathic structure (Fig. 9). The charge-charge interaction on these neighboring oppositely charged residues may stabilize the local amphipathic conformation of Ca²⁺ bound neurocalcin δ . In the case of VILIP-3 and hippocalcin, glutamate, negatively-charged residue, exists at the 21-position in the loop instead of aspartate. Consequently, in analogy with neurocalcin δ , VILIP-3 is expected to conform a similar amphipathic structure; and it may increase the affinity of VILIP-3 for the ER membrane after Ca²⁺-binding and work as a contact surface for mitochondrial cytochrome b5. Regarding the binding to cytochrome b5, it was observed that the N-terminal myristoylation of VILIP-3 is not necessary *in vitro*. However, we suppose that the myristoylated N-terminal end of VILIP-3 may be necessary for the membrane targeting and facilitate the integration of VILIP-3 to the membrane together with the amphipathic structure *in situ*.

Cytochrome b5 is known to function as an electron transfer component in a number of

oxidative reactions. This protein can serve as an electron transfer intermediate between reductases and oxidative enzymes. For example, cytochrome b5 can receive electrons from both NADPH-cytochrome P450 reductase (41–46) and NADH-cytochrome b5 reductase (46), and can transfer electrons to a number of electron acceptor proteins, both model redox acceptors such as cytochrome c (47–49) and natural acceptors, such as cytochrome P450 (48), metmyoglobin (50), methemoglobin (51), and the cyanide-sensitive oxidase involved in stearyl coenzyme A desaturase (46, 52, 53). These proteins carry out the anabolic metabolism of fatty acids, cholesterol, and steroids, as well as the catabolism of xenobiotics and compounds of endogenous metabolism (reviewed in 18, 19). Our results demonstrate for the first time that cytochrome b5 interacts with the Ca^{2+} -binding proteins VILIP-3 and hippocalcin. However, it remains difficult to assign specific physiological functions to VILIP-3 and hippocalcin carried out as a result of the interaction with cytochrome b5, as the terminal enzyme involved in this context is still unknown. One of the natural acceptors, cytochrome P450 enzyme, assumes diverse isoforms. In particular, a number of class II P450 monooxygenases, including microsomal isozymes, have been recognized as utilizing microsomal cytochrome b5 as a source of electrons and thereby forming a multienzyme system referred to as “MMO¹(microsomal monooxygenase)”. Interestingly, cytochrome P450-CYP2j9, expressed primarily in cerebellar Purkinje cells, was isolated from a mouse brain cDNA library (54). This protein metabolizes arachidonic acid to 19-HETE (hydroxyeicosatetraenoic acid), which inhibits the activity of recombinant P/Q-type Ca^{2+} channels, i.e., voltage-gated channels that are known to be expressed preferentially in Purkinje cells and are involved in triggering the release of neurotransmitters. Although it remains unknown whether cytochrome b5 is necessary for the oxidative reaction involving CYP2j9, we postulated that VILIP-3 is involved in regulation of the production of bioactive molecules such as 19-HETE, depending on increase in the intracellular Ca^{2+} concentration;

such processes are thought to occur via interactions with cytochrome b5. VILIP-3 may utilize a microsomal enzyme system in order to enable complex functioning (e.g., synaptic plasticity) in specialized cellular populations such as cerebellar Purkinje cells in the brain. If VILIP-3 is able to act as a Ca^{2+} -dependent regulator of a MMO system, the next question would be whether VILIP-3 enhances or interrupts the enzymatic activity of a MMO in a Ca^{2+} -dependent manner.

Acknowledgements

We thank Dr. Hiroshi Suzuki (the department of biochemistry, Asahikawa Medical College, Asahikawa, Japan) and Dr. Shigetaka Yoshida (the department of anatomy, Asahikawa Medical College, Asahikawa, Japan) for improving our manuscript, Shinichi Chiba (Asahikawa Medical College Central Laboratory for Research and Education, Asahikawa, Japan) for supporting the nucleotide sequence analysis and real time RT-PCR, and Kenji Yamamoto (APRO Life Science Institute, Naruto, Japan) for supporting the amino acid sequence analysis.

REFERENCES

1. Braunewell, K. H., and Gundelfinger, E. D. (1999) *Cell Tissue Res.* **295**, 1-12,
2. Zozulya, S., and Stryer, L. (1992) *Proc. Natl. Acad. Sci. U. S. A.* **89**, 11569-11573
3. Ames, J. B., Ishima, R., Tanaka, T., Gordon, J. I., Stryer, L., and Ikura, M. (1997) *Nature* **389**, 198-202
4. Burgoyne, R. D., and Weiss, J. L. (2001) *Biochem. J.* **353**, 1-12
5. Spilker, C., Gundelfinger, E. D., and Braunewell, K. H. (2002) *Biochim. Biophys. Acta* **1600**, 118-127,
6. Bernstein, H. G., Baumann B., Danos, P., Diekmann, S., Bogerts, B., Gundelfinger, E. D., and Braunewell, K. H. (1999) *J. Neurocytol.* **28**, 655-662
7. Spilker, C., Richter, K., Smalla, K. H., Manahan-Vaughan, D., Gundelfinger, E. D., and Braunewell, K. H. (2000) *Neuroscience* **96**, 121-129
8. Paterlini, M., Revilla, V., Grant, A. L., and Wisden, W. (2000) *Neuroscience* **99**, 205-216
9. Kajimoto, Y., Shirai, Y., Mukai, H., Kuno, T., and Tanaka, C. (1993) *J. Neurochem.* **61**, 1091-1096
10. Kraut, N., Frampton, J., and Graf, T. (1995) *Oncogene* **10**, 1027-1036
11. Guan, K. L., and Dixon, J. E. (1991) *Anal. Biochem.* **192**, 262-267
12. Ho, S. N., Hunt, H. D., Horton, R. M., Pullen, J. K., and Pease, L. R. (1989) *Gene* **77**, 51-59
13. Pfaffl, M. W. (2001) *Nucleic Acids Res.* **29**, e45
14. Lu, G., Lindqvist, Y., Schneider, G., Dwivedi, U., and Campbell, W. (1995) *J. Mol. Biol.* **248**, 931-948
15. Mathews, F. S. (1985) *Prog. Biophys. Mol. Biol.* **45**, 1-56
16. Vijay-Kumar, S., and Kumar, V. D. (1999) *Nat. Struct. Biol.* **6**, 80-88

17. Ermilov, A. N., Olshevskaya, E. V., and Dizhoor, A. M. (2001) *J. Biol. Chem.* **276**, 48143-48148
18. Schenkman, J. B., and Jansson, I. (2003) *Pharmacol. Ther.* **97**, 139-152
19. Vergères, G., and Waskell, L. (1995) *Biochimie* **77**, 604-620
20. Garrett, R. M., Bellissimo, D. B., and Rajagopalan, K. V. (1995) *Biochim. Biophys. Acta* **1262**, 147-149
21. Guiard, B., and Lederer, F. (1977) *Eur. J. Biochem.* **74**, 181-190
22. Cho, H. P., Nakamura, M. T., and Clarke, S. D. (1999) *J. Biol. Chem.* **274**, 471-477
23. Cho, H. P., Nakamura, M., and Clarke, S. D. (1999) *J. Biol. Chem.* **274**, 37335-37339
24. Zhu, H., Qiu, H., Yoon, H. W., Huang, S., and Bunn, H. F. (1999) *Proc. Natl. Acad. Sci. U. S. A.* **96**, 14742-14747
25. Ivings, L., Pennington, S. R., Jenkins, R., Weiss, J. L., and Burgoyne, R. D. (2002) *Biochem. J.* **363**, 599-608
26. O'Callaghan, D. W., Ivings, L., Weiss, J. L., Ashby, M. C., Tepikin, A. V., and Burgoyne, R. D. (2002) *J. Biol. Chem.* **277**, 14227-14237
27. Strittmatter, P., Hackett, C. S., Korza, G., and Ozols, J. (1990) *J. Biol. Chem.* **265**, 21709-21713
28. Porter, T. D. (1991) *Trends Biochem. Sci.* **16**, 154-158
29. Okada, Y., Frey, A. B., Guenther, T. M., Oesch, F., Sabatini, D. D., and Kreibich, G. (1982) *Eur. J. Biochem.* **122**, 393-402
30. Anderson, D. J., Mostov, K. E., and Blobel, G. (1983) *Proc. Natl. Acad. Sci. U. S. A.* **80**, 7249-7253
31. Mitoma, J., and Ito, A. (1992) *EMBO J.* **11**, 4197-4203
32. Enoch, H. G., Fleming, P. J., and Strittmatter, P. (1979) *J. Biol. Chem.* **254**, 6483-6488
33. Arinc, E., Rzepecki, L. M., and Strittmatter, P. (1987) *J. Biol. Chem.* **262**, 15563-15567

34. Visser, L., Robinson, N. C., and Tanford, C. (1975) *Biochemistry* **14**, 1194-1199
35. Vergeres, G., Ramsden, J., and Waskell, L. (1995) *J. Biol. Chem.* **270**, 3414-3422
36. Takagaki, Y., Radhakrishnan, R., Wirtz, K. W., and Khorana, H. G. (1983) *J. Biol. Chem.* **258**, 9136-9142
37. Hanlon, M. R., Begum, R. R., Newbold, R. J., Whitford, D., and Wallace, B. A. (2000) *Biochem. J.* **352 Pt 1**, 117-124
38. Tennyson, J., and Holloway, P.W. (1986) *J. Biol. Chem.* **261**, 14196-14200
39. Ivanov, A. S., Skvortsov, V. S., and Archakov, A. I. (2000) *Vopr. Med. Khim.* **46**, 615-625
40. Ladokhin, A. S., Wang, L., Steggles, A. W., Malak, H., and Holloway, P. W. (1993) *Biochemistry* **32**, 6951-6956
41. Bilimoria, M. H., and Kamin, H. (1973) *Ann. N. Y. Acad. Sci.* **212**, 428-448
42. Enoch, H. G., and Strittmatter, P. (1979) *J. Biol. Chem.* **254**, 8976-8981
43. Hildebrandt, A., and Estabrook, R. W. (1971) *Arch. Biochem. Biophys.* **143**, 66-79
44. Iyanagi, T., Makino, N., and Mason, H. S. (1974) *Biochemistry* **13**, 1701-1710
45. Omura, T., and Takesue, S. (1970) *J. Biochem. (Tokyo)* **67**, 249-257
46. Oshino, N., Imai, Y., and Sato, R. (1971) *J. Biochem. (Tokyo)* **69**, 155-167
47. Hara, T., and Minakami, S. (1971) *J. Biochem. (Tokyo)* **69**, 317-324
48. Jansson, I., and Schenkman, J. B. (1977) *Arch. Biochem. Biophys.* **178**, 89-107
49. Staron, K., and Kaniuga, Z. (1974) *Acta Biochim. Pol.* **21**, 55-60
50. Livingston, D. J., McLachlan, S. J., La Mar, G. N., and Brown, W. D. (1985) *J. Biol. Chem.* **260**, 15699-15707
51. Hultquist, D. E., Dean, R. T., and Douglas, R. H. (1974) *Biochem. Biophys. Res. Commun.* **60**, 28-34
52. Holloway, P. W., and Katz, J. T. (1972) *Biochemistry* **11**, 3689-3696

53. Holloway, P. W., and Wakil, S. J. (1970) *J. Biol. Chem.* **245**, 1862-1865
54. Qu, W., Bradbury, J. A., Tsao, C. C., Maronpot, R., Harry, G. J., Parker, C. E., Davis, L. S., Breyer, M. D., Waalkes, M. P., Falck, J. R., Chen, J., Rosenberg, R. L., and Zeldin, D. C. (2001) *J. Biol. Chem.* **276**, 25467-25479
55. Kyte, J., and Doolittle, R. F. (1982) *J. Mol. Biol.* **157**, 105-132

FOOTNOTE

**to whom correspondence should be addressed: Department of Pathology, Asahikawa Medical College, Midorigaoka Higashi 2-1, Asahikawa, Hokkaido, 078-8510, Japan. Tel.: 81-166-68-2381; FAX: 81-166-68-2389; E-mail: oiken@asahikawa-med.ac.jp

“The nucleotide sequences for mouse VILIP-3 gene, mouse hippocalcin gene, and mouse microsomal cytochrome b5 gene have been deposited in the GenBank database under GenBankAccession Number AF085192, AB015199, and AK013210, respectively. The amino acid sequences of mouse VILIP-3, mouse hippocalcin, bovine neurocalcin δ , and mouse microsomal cytochrome b5 can be accessed through NCBI Protein Database under NCBI Accession # NP_057886, NP_034601, NP_776823, and NP_080073, respectively. The atomic coordinates for the crystal structure of recombinant bovine neurocalcin δ are available in the Research Collaboratory for Structural Bioinformatics Protein Databank under PDB # 1BJF (16).”

¹The abbreviations used are: NCS, neuronal calcium sensor; MMO, microsomal monooxygenase; ER, endoplasmic reticulum; VILIP-3 and V3, visinin-like protein-3; HPCA, hippocalcin; b5, microsomal cytochrome b5; M, c-Myc; F, 3 \times FLAG; Y, EYFP (enhanced yellow-green variant of the *Aequorea Victoria* green fluorescent protein); IPTG, isopropyl-1-thio- β -D-galactoside; GST, glutathione S-transferase; GS4B, glutathione Sepharose 4B; HEPES, 2-[4-(2-hydroxyethyl)-1-piperazinyl] ethanesulfonic acid; CHAPS, 3-[(3-cholamidopropyl) dimethylammonio]-1-propanesulfonate.

FIGURE LEGENDS

Fig. 1. **Relative quantification of murine VILIP-3 mRNA in tissues and cell lines by real-time RT-PCR.** Real-time PCR was performed using a LightCycler system. The single strand cDNAs obtained by reverse transcription from tissues and cell lines were used as templates for real-time PCR. Each histogram indicates the relative expression ratio. **A**, Expression levels of VILIP-3 mRNA in tissues. The control tissue is brain tissue. β -actin was used as a reference gene. **B**, Expression levels of VILIP-3 mRNA in cell lines. The control cell line is BV2. GAPDH was used as a reference gene.

Fig. 2. **Summary of constructs used in the present study.** Schematic representations are, **A**, microsomal cytochrome b5 derivatives; **B**, VILIP-3 derivatives; and **C**, hippocalcin fused to EYFP¹. Amino acid sequences of each construct are shown by bars. Abbreviations used for each construct are indicated on the right or the left side of each bar, and bold indicates the construct of wild-type. The numerals shown above the bars are amino acid positions of each proteins. b5, cytochrome b5; M, c-Myc epitope; F, 3 \times FLAG; GST, glutathione S-transferase; V3, visinin-like protein-3; Y, EYFP; HPCA, hippocalcin.

Fig. 3. **GST pull-down experiment with GST-VILIP-3 fusion proteins.** Silver-stained 2-DE gel protein profiles are shown. FP refers to the fusion proteins used for the pull-down assay, and LB indicates lysis buffer conditions. B6RVTC1 cell were lysed in the presence or absence of calcium. The lysates were pulled down by GST-tagged protein bound to GS4B¹ beads. The pull-down samples were separated by 2-DE gels. Each panel indicates the profile of the sample pulled down by the following: **A**, GST-V3-bound GS4B beads in the presence of calcium, **B**, GST-V3-bound GS4B beads in the absence of calcium, and **C**, GST-bound GS4B beads in the presence of calcium. Molecular weight markers are shown in the right side of each panel, and approximate isoelectric points are indicated in the upper side of each panel. Spot (a) appeared only in the presence of calcium and GST-V3. Other major spots were

estimated based on molecular weight and isoelectric point as follows: (b) GST-V3, (c) endogenous GST from B6RVTC1 cells, (d) recombinant GST.

Fig. 4. Identification of spots on 2-DE gels, obtained by the pull-down assay in the presence of calcium. **A**, The panel indicates CBB-stained 2-DE gels obtained from duplicate samples subjected to the same conditions as those described in Fig. 3A. An interesting spot (a) was also detected on the gel. The gel pieces from the spot (a) were digested using trypsin and were subjected to fingerprinting peptide mapping. N-terminal amino acid analysis identified the spot as murine microsomal cytochrome b5. **B**, The amino acid sequence of cytochrome b5 is shown. Single-underlined sequences indicate an identified polypeptide in the N-terminal amino acid analysis. A dotted sequence indicates a Pro-containing hinge region linking the heme-binding globular domain and the C-terminal hydrophobic domain. The double-underlined region was found within the hydrophobic core of the ER¹ membrane. Bold italics indicate the VILIP-3 binding region. **C**, Model of the two possible topologies of the membrane anchor of cytochrome b5. HBD, heme-binding domain. VILIP-3 binding residues, black: Pro¹¹⁵, gray. (a) transmembrane model. (b) hairpin model.

Fig. 5. Calcium-dependent interaction between murine VILIP-3 and cytochrome b5. 293T cells were co-transfected with constructs of VILIP-3 and cytochrome b5. The transfectants were lysed in the presence or absence of calcium. Then, the lysates were immunoprecipitated by anti-FLAG agarose beads. The immunoprecipitates were analyzed by Western blotting. The constructs used for co-transfection are indicated on the top of the gel. The lysis buffer condition are indicated below the gel. IP refers to the antibody used for the immunoprecipitation, and WB indicates the antibody used for Western blotting. Molecular weight are shown in the left side of each panel. **A**, V3-F (C-terminal 3×FLAG-tagged VILIP-3) and M-b5 (myc-tagged cytochrome b5) expression vectors were used for co-transfection. **B**, V3-Y (EYFP-tagged VILIP-3), HPCA-Y (EYFP-tagged hippocalcin), and F-b5 (N-

terminal 3×FLAG-tagged cytochrome b5) expression vectors were used for co-transfection. The left two lanes, whole cell lysates; the right four lanes, immunoprecipitated samples.

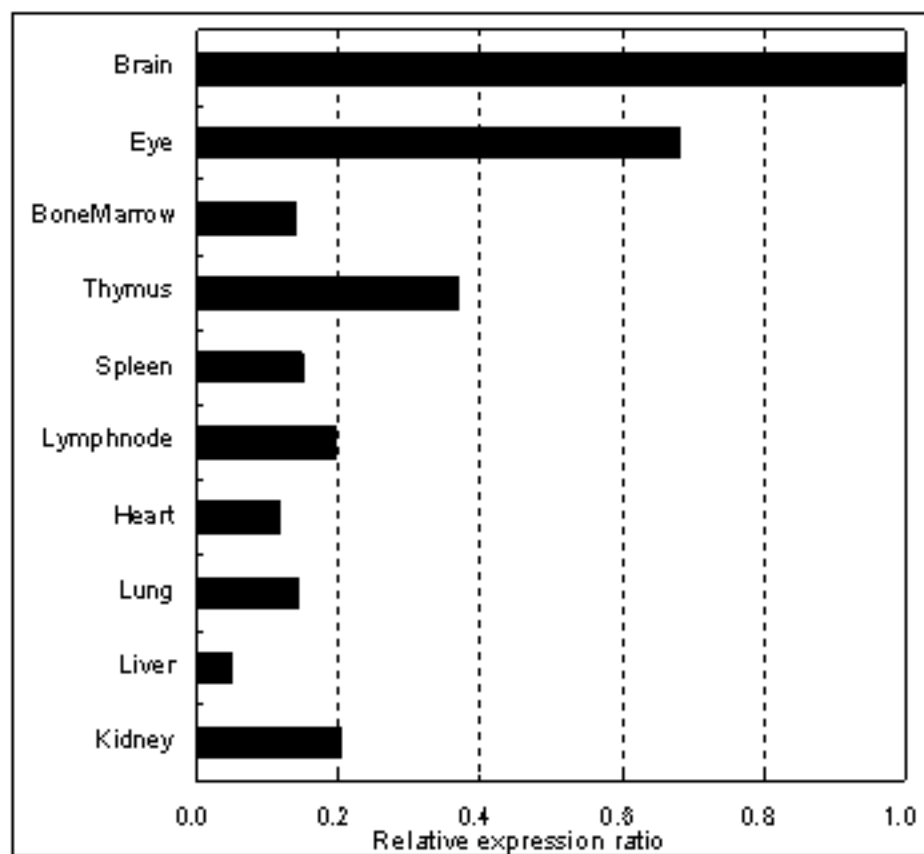
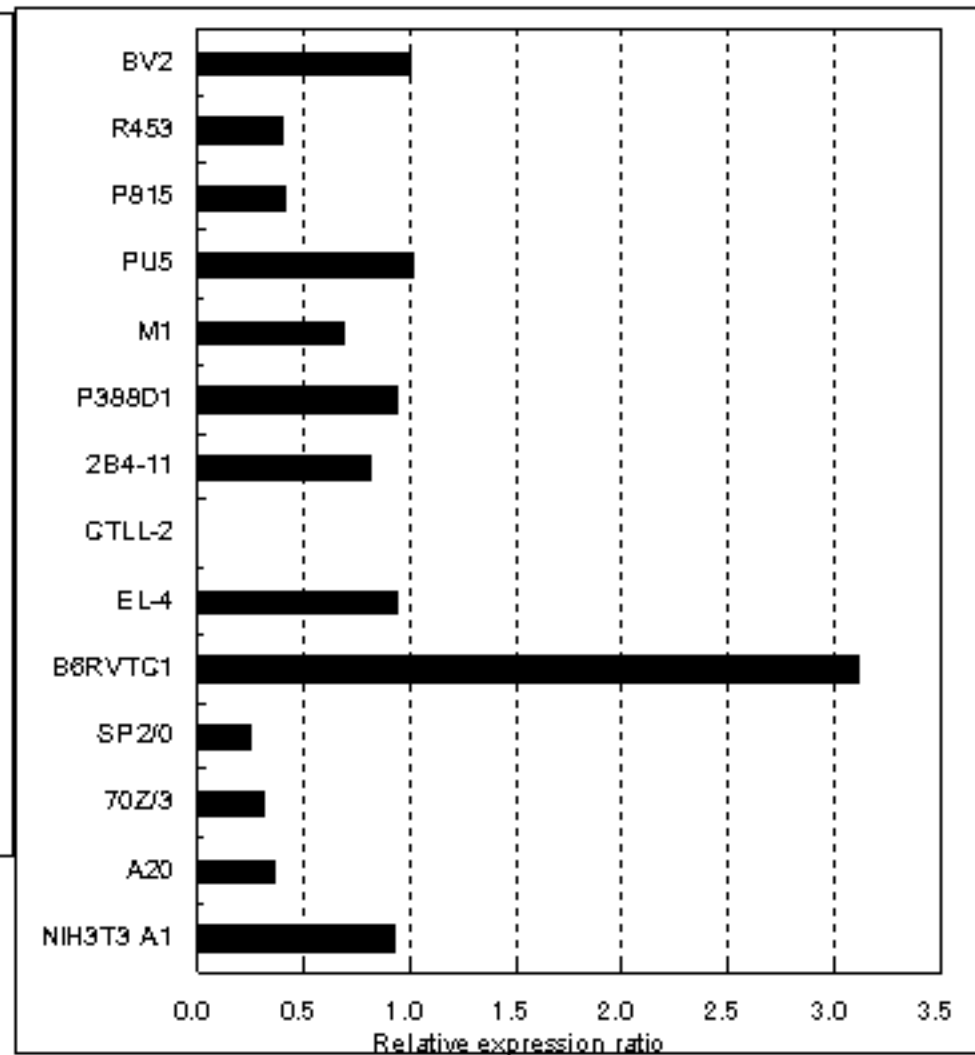
Fig. 6. Identification of the minimal structural requirements for cytochrome b5 interaction with VILIP-3. **A**, The ranges of deletion (the lines at the top) or addition (the lines at the bottom) are shown with the C-terminal sequence of cytochrome b5. The schematic representations of the constructs are summarized in Fig. 2A. **B**, Co-immunoprecipitation assay using V3-F and M-b5-truncated mutants. 293T cells were transfected with each of the expression vectors. All transfectants were lysed in the presence of calcium. The interacting proteins were detected by Western blotting with anti-c-Myc antibody. **C**, *In vitro* binding assay using V3-F and affinity-purified GST-tagged Cytochrome b5 C-terminal truncated mutants. After the incubation of V3-F bound to anti-FLAG agarose beads with GST-cytochrome b5 mutant proteins, the immunocomplexes were analyzed by Western blotting. Anti-GST antibody was used for the detection of GST-cytochrome b5 mutants. **D**, *In vitro* binding assay using V3-F and affinity-purified GST-tagged cytochrome b5 C-terminal polypeptides. The procedure used here was the same as that used for **C**.

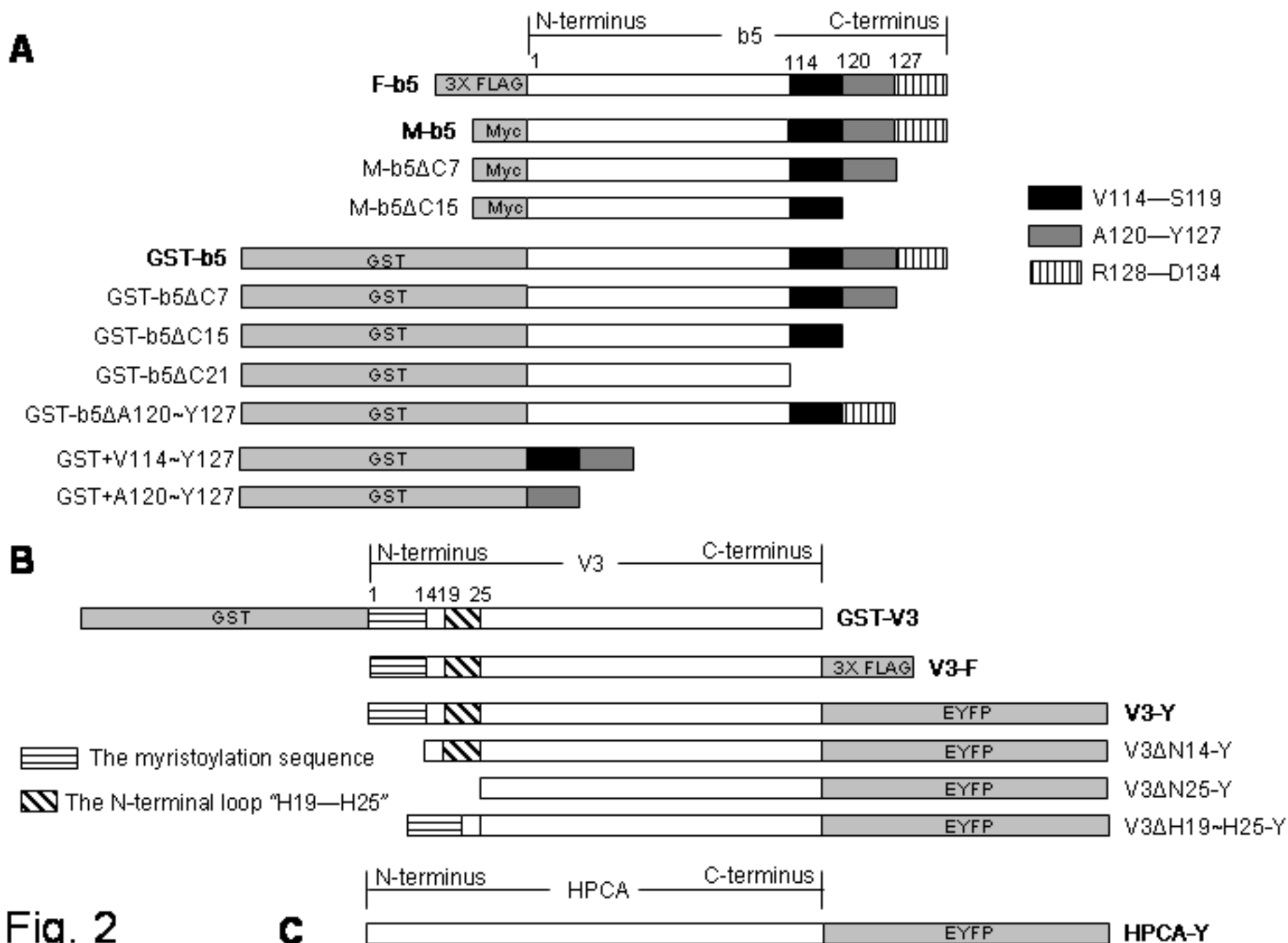
Fig. 7. Identification of the cytochrome b5 binding site of VILIP-3. **A**, N-terminal sequence of murine VILIP-3 and hippocalcin. * indicates amino acid changes of single amino acid-substituted mutants of V3-Y. The arrow underlines indicate the range of deletion in V3ΔN14-Y, V3ΔN25-Y, and V3ΔH19~H25-Y. EF-1 is also indicated by underlining. Underlined bold letters indicate the residues of hippocalcin that differed from those of VILIP-3. The schematic representations of the constructs are summarized in Fig. 2B. **B**, Co-immunoprecipitation assay using F-b5 and single amino acid-substituted mutants of V3-Y. 293T cells were transfected with each expression vector, shown on the top of the gel. All transfectants were lysed in the presence of calcium. The interacting proteins were detected by

Western blotting with anti-EYFP antibody. **C**, Co-immunoprecipitation assay using F-b5 and N-terminal truncated mutants of V3-Y. 293T cells were transfected with each expression vector. All transfectants were lysed in the presence of calcium. The interacting proteins were detected by Western blotting with anti-EYFP antibody. The left four lanes, whole cell lysates; the right four lanes, immunoprecipitated samples.

Fig. 8. Hydrophobicity profiles of mouse VILIP-3 and bovine neurocalcin δ . The hydrophobicity profiles were calculated using the method of Kyte and Doolittle (55). The ordinate indicates hydrophobic index. The first N-terminal loop “H¹⁹ – H²⁵” is shown in a blue box on the profile of VILIP-3. EF-1 and EF-2 are shown in green boxes. The red box indicates the very hydrophobic helix “L⁸⁹ – G⁹⁵”.

Fig. 9. Structural depictions of bovine neurocalcin δ monomer in the Ca²⁺-bound form. PDB#1BJF viewed with CN3D 4.1. The backbone of Ca²⁺-bound bovine neurocalcin δ monomer is shown in blue. The first N-terminal loop “S¹⁹ – H²⁵”, corresponding to the loop “H¹⁹ – H²⁵” in VILIP-3, and the very hydrophobic helix “L⁸⁹ – G⁹⁵” are shown in yellow. (N), N-terminus; (C), C-terminus. **A**, Worm presentation of the bovine neurocalcin δ . **B**, Space-filling model of the neurocalcin δ .

A**B****Fig. 1**



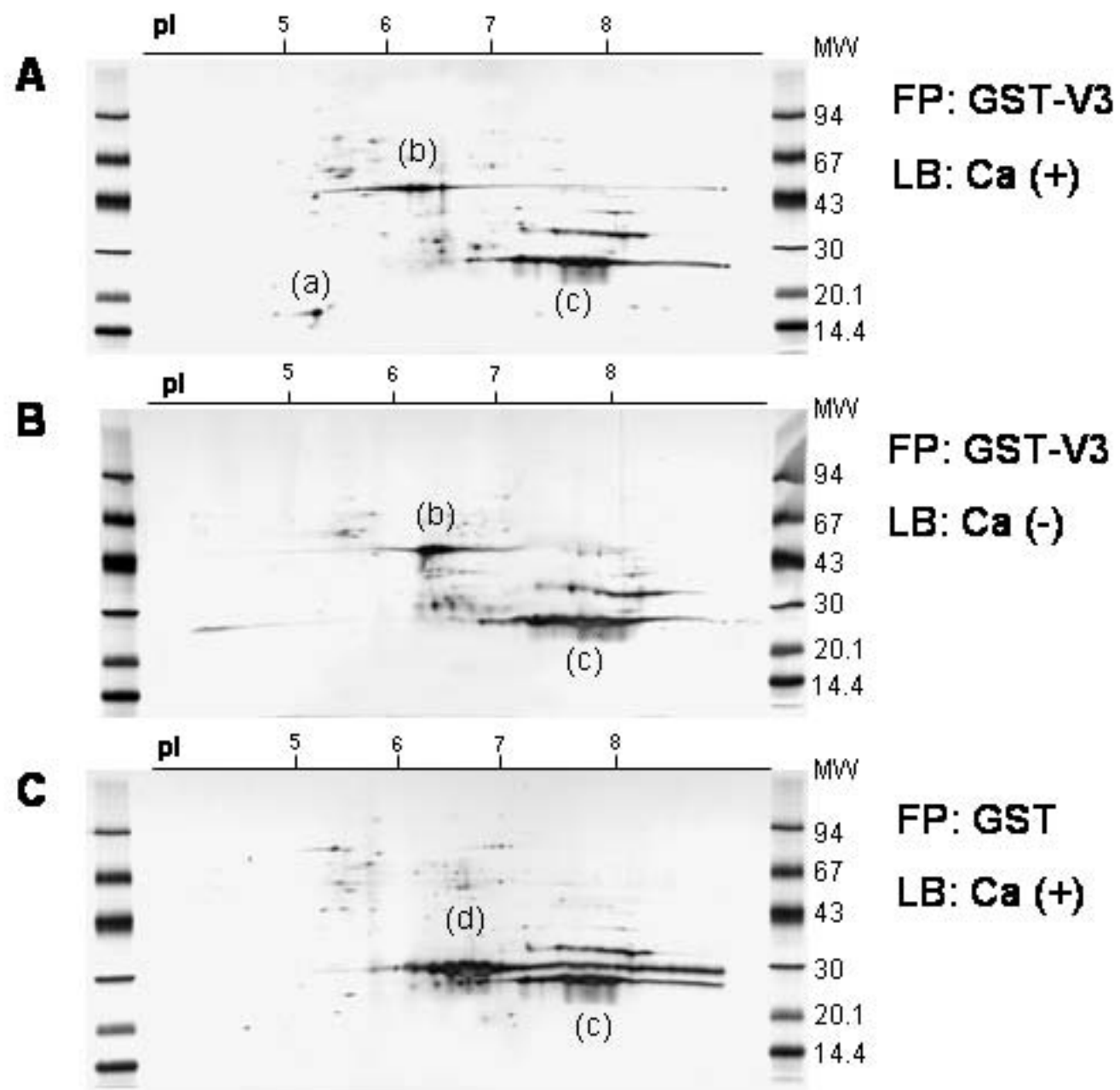


Fig. 3

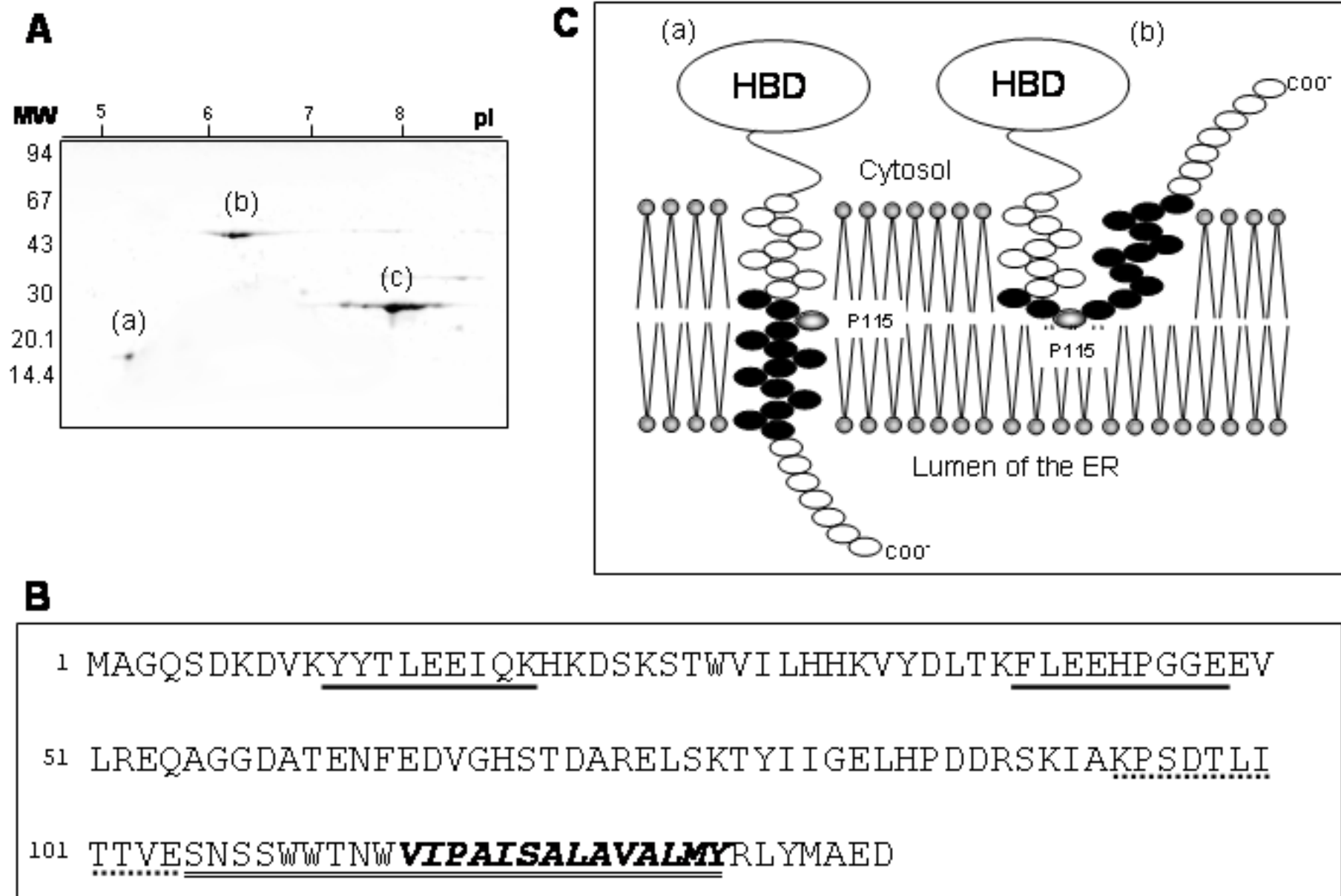


Fig. 4

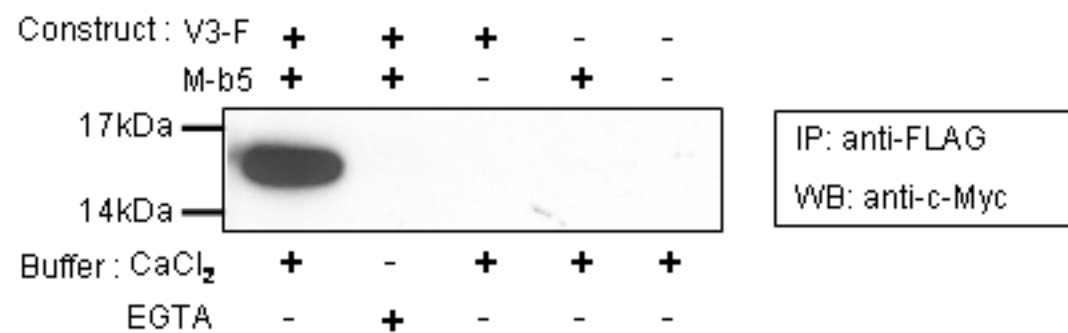
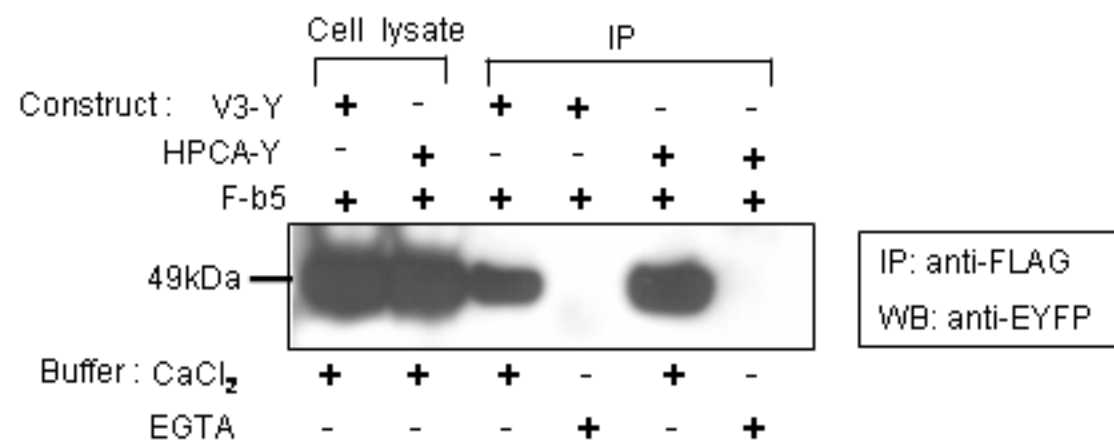
A**B**

Fig. 5

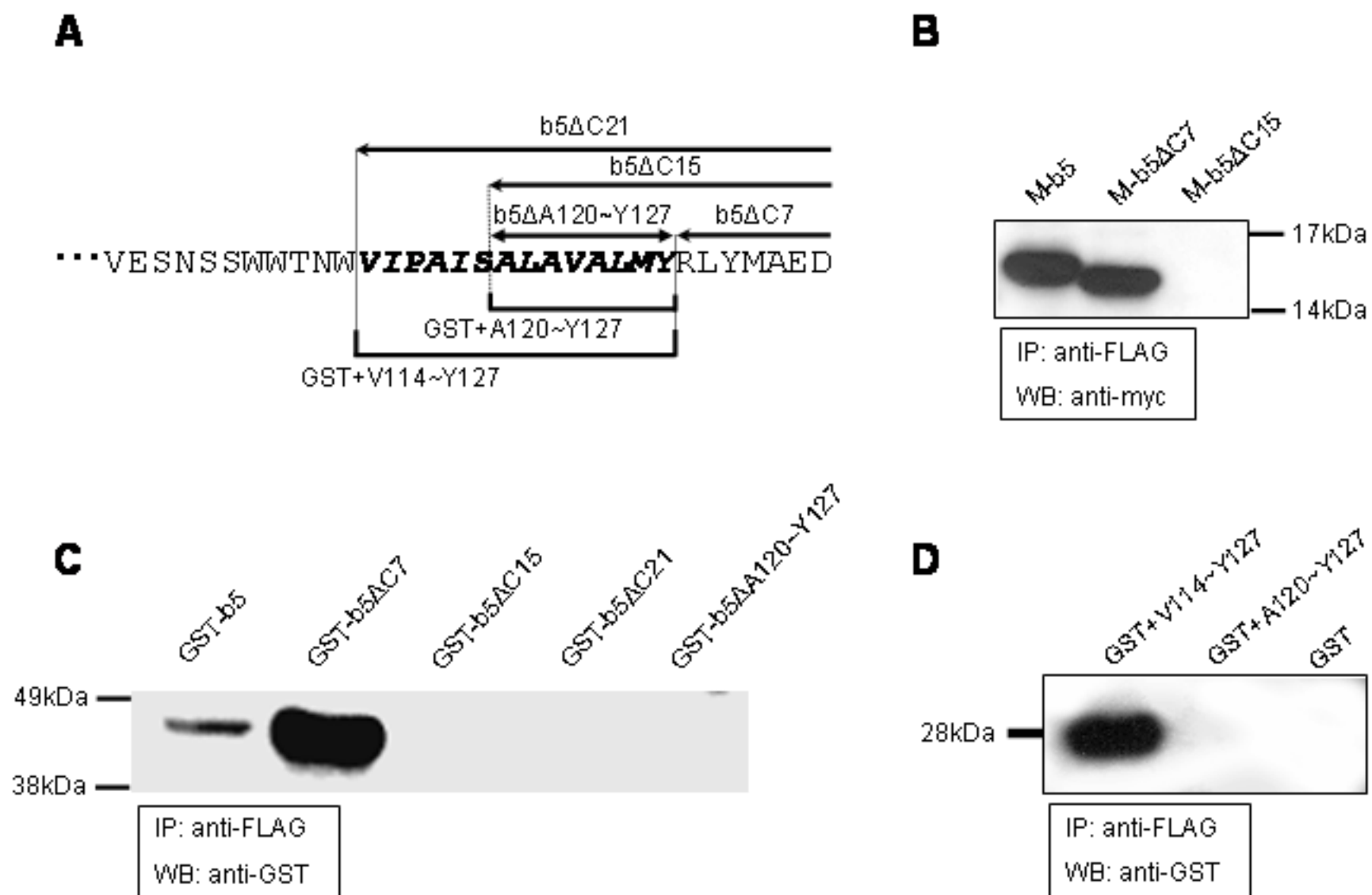
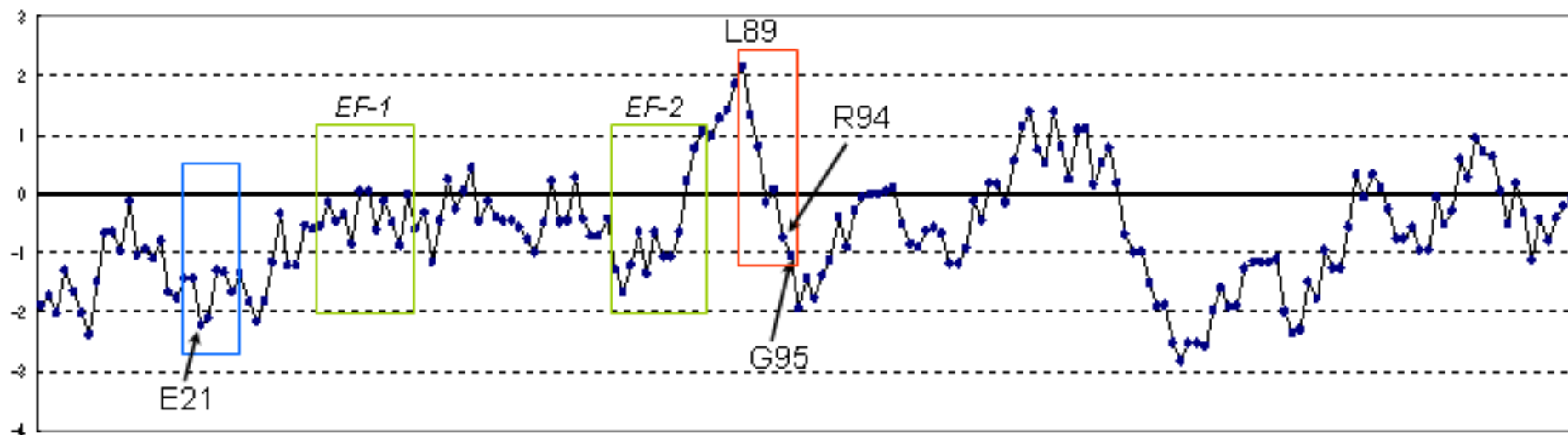


Fig. 6

mouse VILIP-3



bovine neurocalcin δ

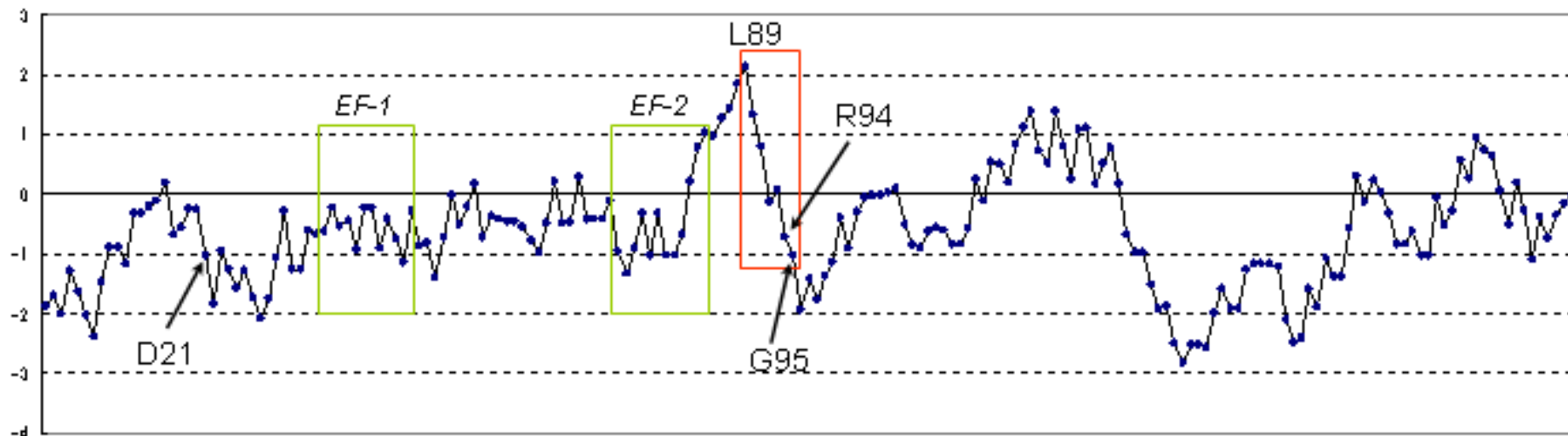


Fig. 8

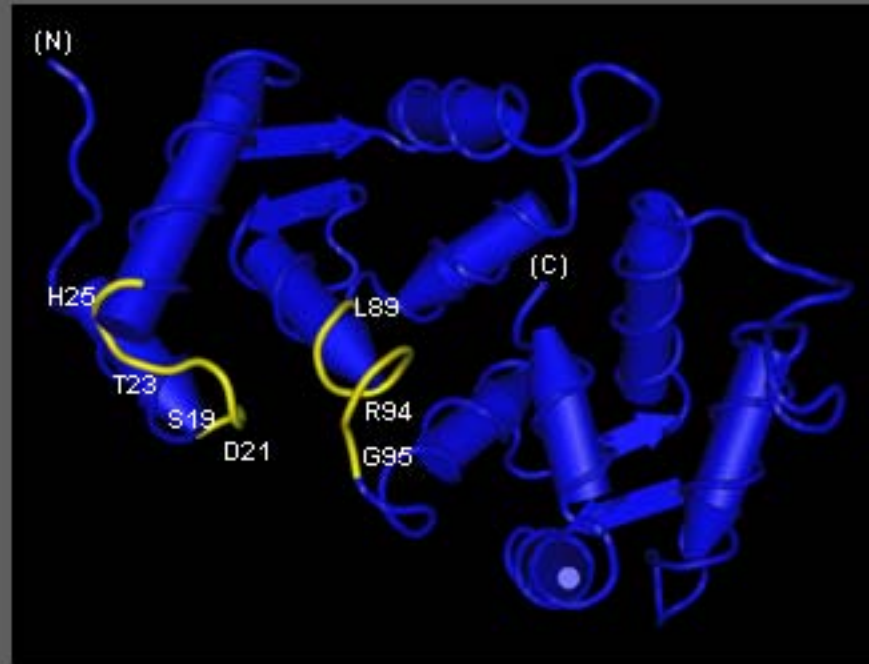
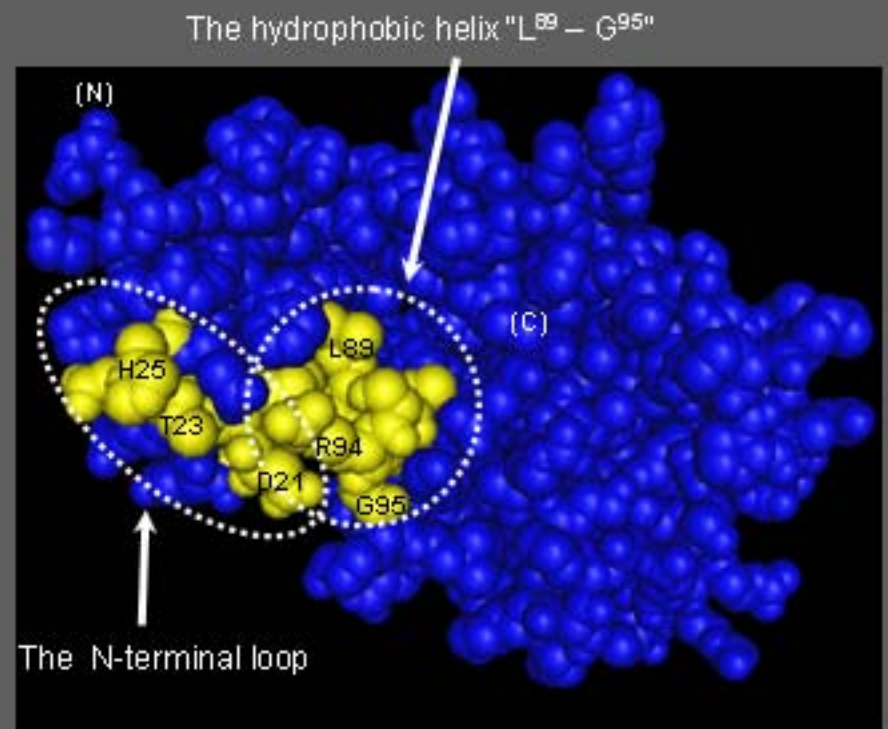
A**B**

Fig. 9